Effect of oxygen penetration in silicon due to nano-indentation

Kausala Mylvaganam and L C Zhang[1]

School of Aerospace, Mechanical and Mechatronic Engineering, The University of Sydney, NSW 2006, Australia

Abstract
This paper aims to explore the effect of O_2 on the nano-indentation of diamond cubic silicon using molecular dynamics simulation. Obtained with the aid of the Tersoff potential for Si–Si interactions and the Morse potential for all other interactions, the results show that on indentation, the O_2 molecule in the appropriate position and orientation dissociates into oxygen atoms, penetrates into the subsurface region and forms chemical bonds with silicon atoms. The penetration of oxygen atoms attracts silicon atoms, causing substantial disorder in the substrate.

(Some figures in this article are in colour only in the electronic version)

1. Introduction

Silicon mono-crystal is a key material for electronic and semiconductor devices. However, when the production of such devices needs a high surface integrity, the associated nano-machining process often causes significant structural changes such as phase transformation and oxidation and thereby changes the mechanical properties of the material. Although quite a number of theoretical [1–4] and experimental [5–10] investigations have looked into the mechanisms of stress-induced phase transformation, the oxidation of silicon during a machining process in a non-vacuum environment has not been studied in detail.

On the other hand, oxidation of silicon without mechanical loading has been studied to a certain extent [11–16]. For example, Kato *et al* [11] reported that back-bond oxidation was energetically favoured. However, they found that this oxidation requires an activation barrier of 0.8–2.4 eV. Bu and Rabalais [12] used the time-of-flight scattering and recoil spectrometry (TOF-SARS) technique to study the chemisorption of O_2 on a Si(100) surface. They found that exposure to O_2 resulted in dissociative chemisorption and at higher coverage the O atoms were adsorbed at the bridge positions between first and second silicon layers. Pasquarello *et al* [13] studied the oxidation of Si(001)–SiO_2 interfaces and observed that three layers of crystalline silicon were oxidized. They also observed that the oxygen diffusion involved an intermediate configuration where the oxygen atom is threefold coordinated by silicon. A recent molecular

dynamics simulation study [17] also showed that O_2 molecules are adsorbed at the bridge positions between the first and second layer, causing substantial disorder of the Si atoms in the first few layers, and the oxygen is threefold coordinated with Si atoms. Recently, in an experimental study on sliding wear, Zhang and Zarudi [18] reported that the oxygen penetrates into the amorphous layer, changes the atomic bonding of silicon, alters the threshold of phase transformation and accelerates wear. However, the mechanism of this chemical process is not yet known.

Nano-indentation involves the penetration of a hard indenter into a sample material and is the simplest mechanical process that can generate a stress field more or less similar to that in a nano-machining process. Thus the present study will investigate the oxidation of silicon during nano-indentation. The molecular dynamics method [19–22] will be used and the silicon surface will be assumed to be oxidation-free before indentation.

2. Modelling

The model used in the simulation is shown in figure 1. The work material (the silicon specimen) is divided into three zones consisting of Newtonian atoms, thermostat atoms and boundary atoms, as in most simulation studies. Boundary atoms are used to restrict the motion of the specimen and thermostat atoms are used to ensure outward heat conduction. To eliminate the boundary effect, the dimension of the control volume of the work material is taken as 10.3 nm × 10.3 nm × 6.5 nm (i.e. 19 unit cells × 19 unit cells

---

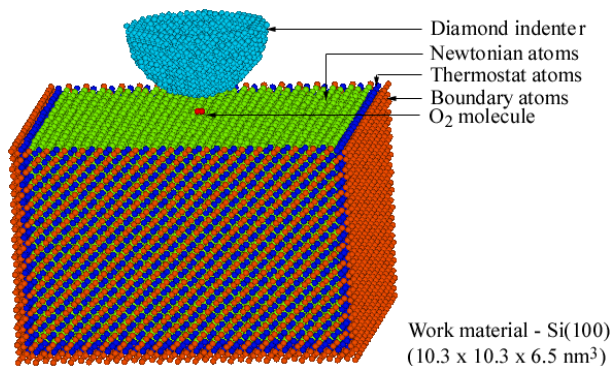[1] Author to whom any correspondence should be addressed.

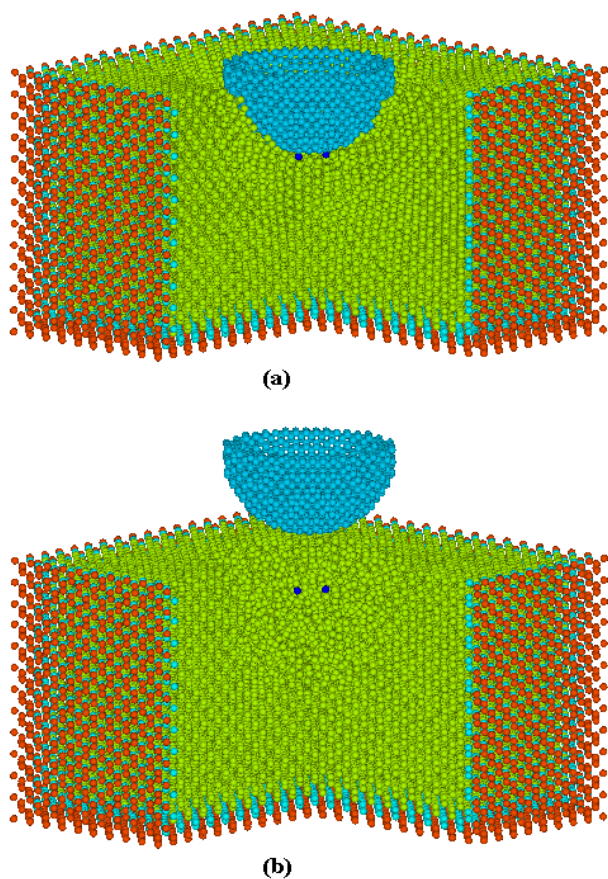**Figure 1.** The molecular dynamics simulation model.

Figure 2. Indentation-induced deformation in the Si substrate with an oxygen molecule (the two black balls under the indenter indicate the two oxygen atoms): (a) at maximum loading, (b) after complete unloading.

× 12 unit cells), containing 36 341 Si atoms. The simulation is done at room temperature with a time step of 2.5 fs, an optimum value for Si as reported elsewhere [23].

The initial substrate–indenter separation is 7 Å and the oxygen molecules are placed in between the silicon substrate and the indenter at different positions. As the space between the substrate and the indenter is only 7.451×10^{-20} cm^3, theoretically in this space at most only one oxygen molecule could be present in the air at standard temperature and pressure. Hence, in this work, we carried out a detailed analysis with one oxygen molecule to mimic the experimental conditions. To capture the effect of the position of the oxygen molecule,

Table 1. Parameters for the Morse potential.

Parameter	Si–O	Si–C	O–O [32]
α (Å^{-1})	1.865	4.6417	2.667
D (kcal mol^{-1})	107.8	100.32	119.12
r_0 (Å)	1.631	1.9475	1.210

the following special cases are specifically considered:

(i) as shown in figure 1, the oxygen molecule is at the centre right below the indenter and 2 Å above the surface;

(ii) as in (i) but 1 Å away from the centre; and

(iii) as in (i) but 5 Å above the surface.

The indentation is done with an inert hemispherical diamond indenter having 1818 atoms. A three-body Tersoff potential [24, 25], which has been used extensively in MD simulation studies of silicon, was employed for the interaction between Si atoms. A two-body Morse potential was used for all other interactions because it has been used successfully for a large number of machining and indentation processes of various materials (silicon, copper and aluminium) involving substrate–tool interaction [1, 23, 26–29]. The Morse potential can be written as

$$V(r_{ij}) = D[e^{-2\alpha(r_{ij}-r_0)} - 2e^{-\alpha(r_{ij}-r_0)}]$$

where $\alpha = 10\sqrt{6.023\,f_{ii}/2D}$ Å at equilibrium and f_{ii} is the second derivative of the potential energy V with respect to the bond length r. For the Si–O bond, the parameter α is calculated using an f_{ii}-value [30] of 9.24 N cm^{-1} which is very close to the value used by Price and Parker [31] in their successful prediction of structures and physical properties of forsterite and ringwoodite, the major polymorphs of Mg$_2$SiO$_4$. The appropriate parameters in the Morse potential are given in table 1.

The potentials used in the calculation, the models chosen for the temperature–kinetic energy conversion, the time step used for numerical integration and the size of the control volume selected were compared with the relevant experimental measurements and shown to be reliable and accurate as discussed in [23, 31].

3. Results and discussion

(i) The O$_2$ molecule was placed laterally (i.e. parallel to the surface) right below the indenter and 2 Å above the surface (figure 1).

Locations of the oxygen atoms at different stages of the indentation process are shown in figure 2. The oxygen molecule dissociated into atoms and both atoms went into the substrate and formed threefold/fourfold coordination with Si atoms. At the early stages, these oxygen atoms were within the first two or three layers of silicon. As the loading proceeded these oxygen atoms went further in, but they were close to the indenter tip and there were no significant changes in the silicon–oxygen coordination. Towards the maximum loading and on unloading, the 'addresses' of the nearest neighbours showed that the oxygen atoms were coordinated with different silicon atoms. However, the oxygen atoms were threefold/fourfold coordinated with silicon atoms throughout loading and unloading.

At the end of the indentation process, the oxygen atoms were found about 8 Å below the surface in the amorphous phase.

The difference in total energy during the latter stages of loading and on unloading of the indentation process with and without oxygen would give the energy released in the formation of new Si–O bonds. This analysis showed that altogether ten new Si–O bonds should have formed. This is higher than the number of Si–O bonds that is deduced by looking at the nearest neighbours. However, we found that there were some Si atoms that would have weak interactions with the penetrated oxygen atoms and this would account for the excess energy.

(ii) The O_2 molecule was 1 Å away from the centre.

During the loading process the oxygen molecule dissociated into atoms but only one oxygen atom went into the substrate and coordinated with silicon atoms. The other oxygen atom went away. The oxygen atom that went in formed threefold/fourfold coordination with silicon atoms as in case (i).

(iii) The O_2 molecule was 5 Å above the surface.

In the initial stages, the O_2 molecule rotated around and then dissociated into atoms, but only one oxygen atom went into the substrate and formed threefold/fourfold coordination with silicon atoms.

The above results indicate that the position and orientation of the oxygen molecule play a key role in the penetration of the oxygen atoms into the substrate.

The structural changes during the loading and unloading of the indentation process when the O_2 is placed right below the indenter are shown in figure 3. It is clear that there is a significant difference in the number of fourfold-, fivefold- and sixfold-coordinated silicon atoms. At the maximum indentation there is a remarkable increase in the number of fivefold-coordinated silicon atoms, which could be an intermediate in the formation of sixfold-coordinated β-tin phase, when the indentation is carried out in the presence of O_2. This is due to the attraction of silicon atoms towards the penetrated oxygen atoms and is confirmed by figure 4, which shows the number of silicon atoms that are within 10 Å of the O atom/dummy O atom. Throughout the indentation process (except at the very beginning) there are more Si atoms around the O atom compared to the number of Si atoms in the same region when the indentation is carried out without O_2 (i.e. in vacuum).

On unloading, as stated by Cheong and Zhang [1], the β-silicon transforms into the amorphous phase and as a result the number of fourfold-coordinated silicon atoms may increase; this is reflected in figure 3(a). The fact that after unloading there are more Si atoms around the oxygen clearly indicates that the oxygen penetration causes damage to the silicon substrate.

4. Conclusions

In summary, the present study has shown that silicon monocrystal can become oxidized during the indentation process; if an oxygen molecule in the atmosphere happens to be below the indenter, the oxidation would damage the subsurface structure of silicon. This explains why oxidation and its associated subsurface damage take place in nano-tribological sliding and precision surfacing processes, such as grinding, polishing and lapping. In these processes the many moving surface asperities
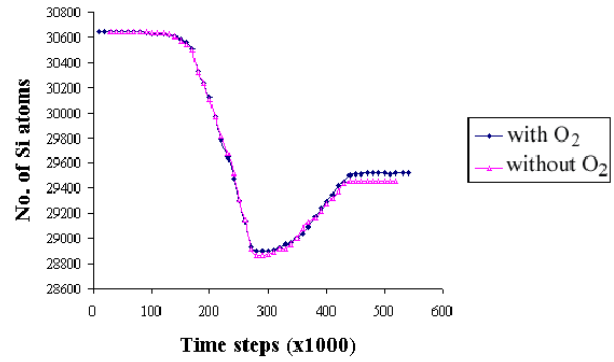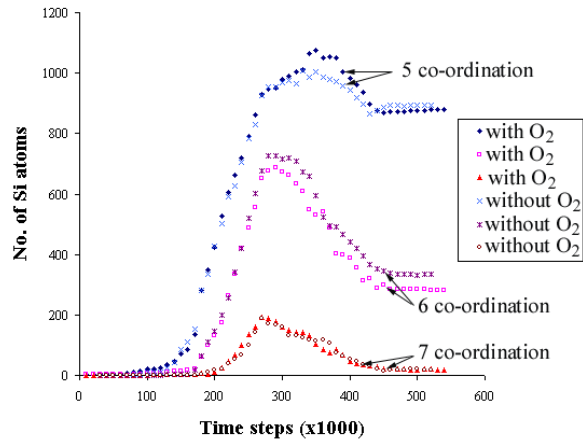
Figure 3. Structural changes of the substrate: (a) compares the number of fourfold-coordinated Si atoms and (b) compares the number of fivefold-, sixfold- and sevenfold-coordinated Si atoms during the indentation process with and without O_2.
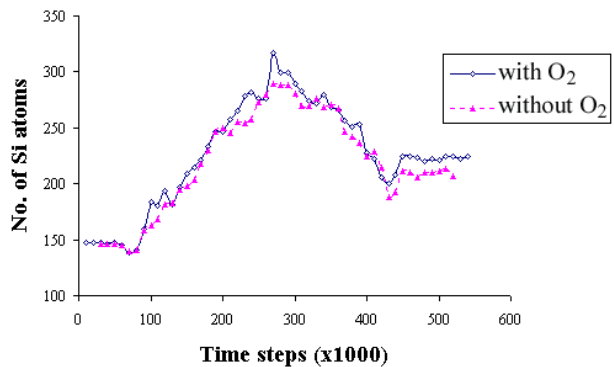

Figure 4. Comparison of the total number of Si atoms around one of the penetrated O atoms/dummy O atoms during the indentation process with and without O_2.

act as abrasive grit and can be viewed as moving indenters; these would greatly increase the chance of oxidation.

The present work concerns the oxidation of an initially clean surface. However, the methodology and the potentials used here can be used directly for analysing the oxidized layer effect by placing a pre-oxidized layer on a pure silicon sample.

References

[1] Cheong W C D and Zhang L C 2000 *Nanotechnology* **11** 1
[2] Pfrommer B G *et al* 1997 *Phys. Rev.* B **56** 6662
[3] Kallman J S *et al* 1993 *Phys. Rev.* B **47** 7705
[4] Chang K J and Cohen M L 1985 *Phys. Rev.* B **31** 7819
[5] Mann A B and van Heerden D 2000 *J. Mater. Res.* **15** 1754
[6] Domnich V and Gogotsi Y 2000 *Appl. Phys. Lett.* **76** 2214
[7] Gogotsi Y, Baek C and Kirscht F 1999 *Semicond. Sci. Technol.* **14** 936
[8] Zarudi I and Zhang L C 1999 *Tribol. Int.* **32** 701
[9] Hu J Z *et al* 1986 *Phys. Rev.* B **34** 4679
[10] Needs R J and Martin R M 1984 *Phys. Rev.* B **30** 5390
[11] Kato K, Uda T and Terakura K 1998 *Phys. Rev. Lett.* **80** 2000
[12] Bu H and Rabalais J W 1994 *Surf. Sci.* **301** 285
[13] Pasquarello A, Hybertsen M S and Car R 1998 *Nature* **396** 58
[14] Ikeda H *et al* 1995 *J. Appl. Phys.* **77** 5125
[15] Uchiyama T, Uda T and Terakura K 1999 *Surf. Sci.* **433–435** 896
[16] Miyamoto Y, Oshiyama A and Ishitani A 1990 *Solid State Commun.* **74** 343
[17] Mylvaganam K and Zhang L C 2002 in preparation
[18] Zhang L and Zarudi I 1999 *Wear* **225–229** 669
[19] Landman U *et al* 1990 *Science* **248** 454
[20] Haile J M 1992 *Molecular Dynamics Simulation* (New York: Wiley)
[21] Hoover W G 1986 *Molecular Dynamics* (Berlin: Springer)
[22] Heermann D W 1986 *Computer Simulation Methods in Theoretical Physics* (Berlin: Springer)
[23] Zhang L and Tanaka H 1999 *JSME Int. J.* A **42** 546
[24] Tersoff J 1989 *Phys. Rev.* B **39** 5566
[25] Tersoff J 1986 *Phys. Rev. Lett.* **56** 632
[26] Komanduri R, Chandrasekaran N and Raff L M 2001 *Phil. Mag.* B **81** 1989
[27] Komanduri R, Chandrasekaran N and Raff L M 2000 *Wear* **242** 60
[28] Komanduri R, Chandrasekaran N and Raff L M 2000 *Wear* **240** 113
[29] Ikawa W *et al* 1991 *Ann. CIRP* **40** 551
[30] Lide D R (ed) 2000–2001 *CRC Handbook of Chemistry and Physics* 81st edn (Boca Raton, FL: Chemical Rubber Company Press)
[31] Price G D and Parker S C 1984 *Phys. Chem. Minerals* **10** 209
[32] Coreno M *et al* 1999 *Chem. Phys. Lett.* **306** 269